Kinetic modeling of liquid phase catalytic alkylation of guaiacol with cyclohexene

Mardelly Kateryne Montañez-Valencia, Cristina Liliana Padró, María Eugenia Sad*, Nicolás Maximiliano Bertero*

Catalysis Science and Engineering Research Group (GICIC), INCAPE, UNL-CONICET, Predio CCT Conicet, Paraje El Pozo, Santa Fe 3000, Argentina

A B S T R A C T

The kinetics of the liquid-phase alkylation of guaiacol (G) with cyclohexene (CH) over Amberlyst 36 resin was studied using Langmuir–Hinshelwood–Hougen–Watson (LHHW) heterogeneous kinetic models. Catalytic tests were performed in a batch reactor, in solvent-less conditions, at 363 K, 1 bar, 600 RPM, using a G:CH molar ratio equal to 5 with a total volume of 30 ml and 1.5 g of solid catalyst. The alkylation of *G* with CH formed cyclohexyl-2-methoxyphenylether (CHMPE) by O-alkylation and cyclohexyl-2-methoxyphenol isomers (CHMP) by C-alkylation. Furthermore, CHMPE isomerizated into CHMP. A negligible amount of cyclohexylcyclohexene (CHC) was observed by dimerization of CH. Among these products, CHMP are important intermediaries for the production of resins, antioxidants, drugs, polymeric additives, agrochemicals, etc.

Several LHHW kinetic models, varying the rate limiting step of reactions, were proposed in order to elucidate a reaction mechanism. The fitting of experimental data was performed consecutively by: (1) a stochastic optimization method and (2) by nonlinear regression, using the Levenberg–Marquardt algorithm, reducing the probability of reaching local minima in the objective function. The selected kinetic model considers that: (a) the rate limiting step for both the O-alkylation and C-alkylation is the surface chemical reaction between adsorbed G and adsorbed CH; (b) the adsorption of the O-alkylated products is the rate limiting step for the isomerization into C-alkylated products. Finally, this kinetic model that fits experimental data appreciably well from both physical and statistical point of view, suggests that CH adsorbs stronger than G over Amberlyst 36 catalyst.

1. Introduction

Alkylation of aromatics is a useful reaction to produce a width variety of valuable chemicals. Traditionally, Friedel-Crafts alkylation have been performed using BF_3, $AlCl_3$, $SnCl_4$ and Brønsted mineral acids such as H_3PO_4, HF or H_2SO_4 which generate problems of high toxicity, corrosion, and waste disposal [1]. Therefore, the replacement by alternative environmentally friendly solvent-free routes using solid catalysts is highly desirable. Particularly, alkylation of guaiacol (2-metoxyphenol) with cyclohexene leads to valuable products since it allows to create a new C-O bond to form cyclohexyl-2-methoxyphenylether (CHMPE, O-alkylation product) which is used as intermediate in the synthesis of perfumes [2] or a new C-C bond directly attached to the aromatic ring to yield the C-alkylation isomers, cyclohexyl-2-methoxyphenol (CHMP). The C-alkylation products are valuable and important intermediaries to produce resins, antioxidants, drugs, dyes, polymeric additives, agrochemicals, and antiseptics [3].

Both guaiacol (G) and cyclohexene (CH) could be obtained from biomass. G is one of the more abundant compounds yielded from the decomposition of lignin [4] and CH, though is mainly derived from petrochemical fractions, could be produced from cyclohexanol obtained by pyrolysis of lignocellulosic materials [5] or from the same guaiacol [6].

The reaction network for the alkylation of guaiacol with cyclohexene is shown in Fig. 1. Guaiacol reacts with cyclohexene mainly through two parallel reactions: O-alkylation (OA) of G to form the CHMPE and C-alkylation (CA) in the aromatic ring leading to the formation of CHMP isomers. In addition, the isomerization of CHMPE to CHMP can also take place over catalytically active acid sites. Moreover, cyclohexylcyclohexene (CHC), the CH dimer, can be produced from two CH molecules.

Previous studies of guaiacol alkylation in liquid phase using heterogeneous catalysis have concluded that Brønsted acid sites efficiently catalyze this reaction. Indeed, sulfated zirconia, Amberlyst 15, dodecatungstophosphoric acid supported, Filtron-24 and Indiol-130 were previously tested by Yadav et al. [3,7] and they found that selectivity to both O- and C- alkylated compound could be managed by se-
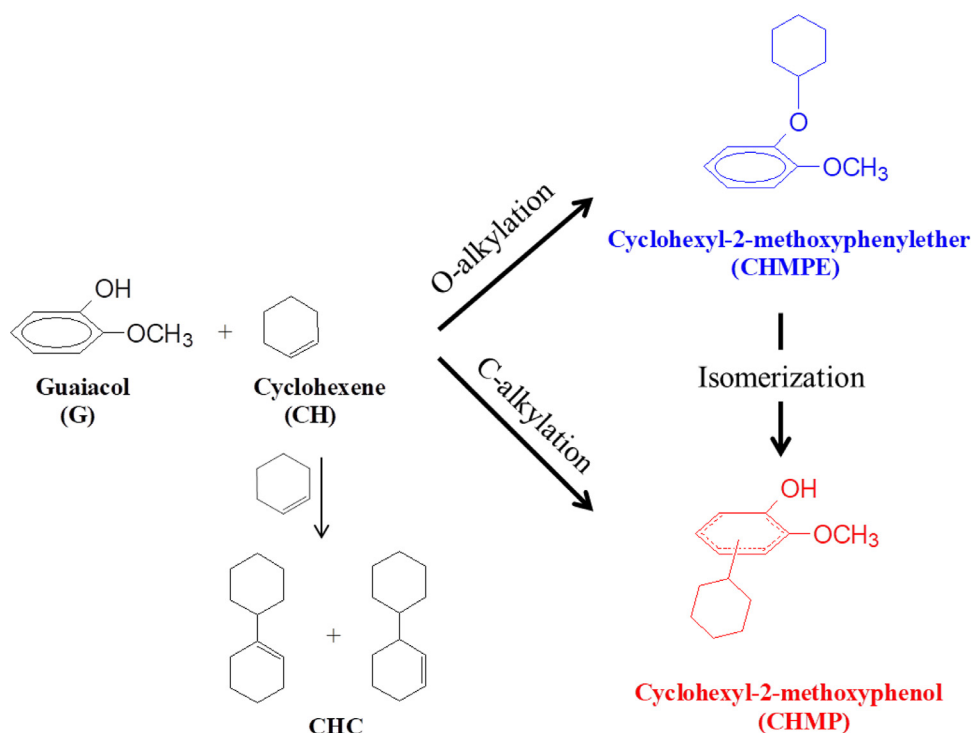
Fig. 1. Reaction network for guaiacol alkylation with cyclohexene over acid catalysts.

lection of appropiate reaction conditions. However, the reaction rates towards the two main routes, i.e. O- and C-alkylation, were no property discussed. In a preliminary study, the catalytic behavior of solids with Lewis, Brønsted or both types of acid sites was tested, proving that the resin Amberlyst 36 highly favored C-alkylation route (Table SM.1 in Supplementary Material). However, a mechanism for the formation of C-alkylated product from G and CH has not been reported yet. In general, it is possible to find three kinds of kinetic models in the literature: (i) pseudo-homogeneous, (ii) LHHW models and (iii) non-stationary kinetic models. In the particular case of alkylation reactions the most widely used kinetic models are based on LHHW kinetics. However, if several assumptions and simplifications are done in the adsorption term (denominator in LHHW expressions), these models can be converted into a pseudo-homogeneous kinetic model with a limited comprehension of the heterogenous process [2,3]. In the present work, we have selected a promising catalyst to favor the CHMP formation (Amberlyst 36) and tested several Langmuir–Hinshelwood–Hougen–Watson (LHHW) kinetic models to propose a mechanism for explaining the formation of C-alkylation products. LHHW kinetics were chosen for describing the alkylation of guaiacol with cyclohexene due to the fact that these models fit appreciably well a commitment between explanation of the catalytic phenomenon and computational cost for having a moderate number of kinetic parameters.

2. Experimental

A commercial Amberlyst 36 resin was used as catalyst. Prior to the characterization and catalytic tests, it was dried at 353 K for 12 h. The concentration of acid sites in Amberlyst 36 was determined by potentiometric titration reported elsewhere [8] using a pH electrode and a Trans Instrument HP3040 potentiometer.

The alkylation of G (Sigma-Aldrich, ≥ 99%) with CH (99%, Sigma) was carried out in liquid phase in a glass batch reactor, at atmospheric pressure with a constant stirring rate (600 RPM). The reactor was immersed in a glycerin bath and connected to a condenser where a cold-water stream (278 K) was kept flowing to avoid the evaporation of cyclo-

hexene. The reaction was conducted without a solvent, at 363 K, using a G:CH molar ratio equal to 5 with a total volume of 30 ml and 1.5 g of solid catalyst. Samples were withdrawn periodically, from the reaction mixture, filtered, mixed with cyclohexane (external standard) and analyzed in an Agilent 6850 gas chromatograph equipped with a 30 m HP5 capillary column (internal diameter: 0.32 mm, film thickness: 0.25 μm) and a flame ionization detector (FID). The identification of CHMPE and CHMP isomers (non-commercially available products) was carried out by gas chromatography–mass spectrometry and 1H NMR spectroscopy using a Thermo Scientific ISQ QD Simple Quadrupole GC-MS equipped with a 30 m TR-5MS column (inner diameter: 0.25 mm, film thickness: 0.25 μm) and a Bruker Advance 300 MHz spectrometer and CDCl$_3$ as a deuterated solvent, respectively. The conversion of cyclohexene (X_{CH}), i product yield (η_i) and carbon balance (CB) were calculated as shown in Section SM.1 of Supplementary Material.

Preliminary catalytic tests were performed using different solid acid catalysts with Brønsted acid sites such as Amberlyst 36, ZrO_2-SO_4, Nb_2O_5-SO_4 and HZSM5. Amberlyst 36 was selected as the most active and selective catalyst to promote the C-alkylation of guaiacol with cyclohexene at the reaction conditions used here (Section SM.2 of Supplementary Material).

Before considering any kinetic modeling, the absence of external and intraparticle mass transfer limitations was verified using well-known criteria [9,10], also widely employed for acid-catalyzed liquid-phase reactions [11,12]. More details about these calculations are provided in Section SM.3 of Supplementary Material. Catalyst stability during the alkylation of guaiacol with cyclohexene was verified by performing two consecutive reactions using the same Amberlyst 36. After the first 8 h reaction cycle, the catalyst was recovered, washed, dried at 353 K for 12 h and tested in a new reaction cycle.

Regarding the kinetic modeling, the system of differential equations describing mass balances for the species in liquid phase was solved numerically by nonlinear parameter estimation using the Runge–Kutta–Merson algorithm combining two different methodologies. The purpose of this was to minimize the probability of reaching local optima in objective function S when only a deterministic method is used, and poor ini-

tial guess values are provided [13]. For instance, Levenberg-Marquardt algorithm is the most used deterministic gradient-based method exhibiting rapid quadratic convergence, though is very sensitive to the starting guess values. Therefore, the fitting of experimental data was performed by: (1) an stochastic optimization method (or adaptive random search) [14], which scans the entire parameter space and theoretically converges to the global minimum after a relatively high computational time [15], useful for obtaining good initial estimates and (2) by nonlinear regression, using the Levenberg–Marquardt algorithm starting from the results of the stochastic method (after 10 min run). Thus, the probability of reaching local minima in the objective function is significantly reduced than using only the deterministic method.

The parameter estimation was performed by minimizing the objective function of Eq. (1):

$$S = \sum_{t} \left(C^*_{i,t} - C^{*CALC}_{i,t} \right)^2 \tag{1}$$

where $C^*_{i,t}$ and $C^{*CALC}_{i,t}$ are the experimental and calculated relative concentrations, respectively, of i compound at the reaction time t.

The coefficient of determination (r^2) gives the fitting quality (i.e., the percentage of explanation of the total data variation around the average observed value) and was estimated by Eq. (2):

$$r^2 = \frac{\sum_{i=1}^{n} \left(C^{*CALC}_i - \overline{C^*} \right)^2}{\sum_{i=1}^{n} \left(C^*_i - \overline{C^*} \right)^2} \tag{2}$$

where $\overline{C^*}$ is the average relative concentration, while C^*_i and C^{*CALC}_i are the experimental and predicted values, respectively.

The model adequacy and the discrimination between models were carried out using the model selection criterion (MSC), according to Eq. (3):

$$MSC = ln\left[\frac{\sum_{i=1}^{n} \left(C^*_i - \overline{C^*} \right)^2}{\sum_{i=1}^{n} \left(C^*_i - C^{*CALC}_i \right)^2} \right] - \left(\frac{2p}{n} \right) \tag{3}$$

where n is the number of experimental data and p is the number of parameters fitted. When models are compared with different number of parameters p, the most significant model is that which leads to the highest MSC value.

3. Results and discussion

The surface area (S_{BET}) and the mean pore diameter of Amberlyst 36 resin (provided by the manufacturer) were 33 m²/g and 240 Å, respectively. The concentration of Brønsted sites acid determined by potentiometric titration was 4.82 mmol H⁺/g.

Fig. 2 shows the temporal evolution of cyclohexene conversion (X_{CH}) and yields (η_i). CH rapidly reacts with G to reach almost total conversion at 4 h of reaction. The C-alkylated products, i.e. CHMP, were the main products formed, although the formation of the O-alkylated product (CHMPE) was also important at low reaction times. The CHMPE yield curve reached a maximum at about 1 h and then decreased suggesting its isomerization to CHMP as proposed in Fig. 1. Cyclohexylcyclohexene (CHC), the dimer formed from two CH molecules was also detected; however, its yield (η_{CHC}) was always lower than 3%. Carbon balance was higher than 95 % during the entire reaction.

The significance of liquid-solid mass transfer on the kinetic regime for the reaction operating conditions used in this work was investigated by applying the quantitative criterion described by Ramachandran and Chaudhari [10]. The absence of intraparticle diffusion limitations was
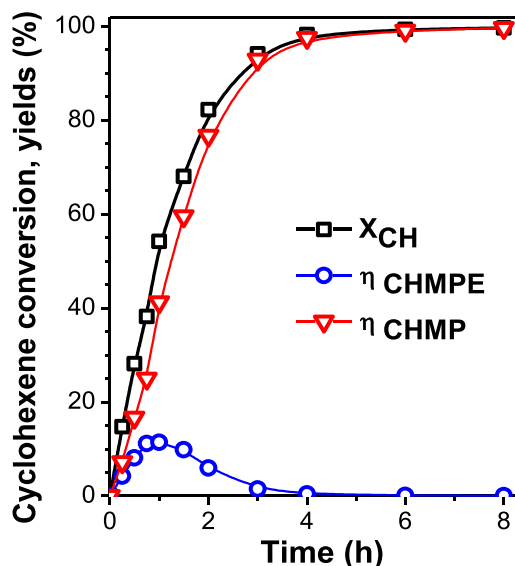

Fig. 2. CH conversion (X_{CH}) and product yields as a function of time [363 K, C_{CAT} = 50 g/L, G:CH 5:1 molar].

also checked by using the Weisz Prater criterion [11]. Based on these calculations performed in Section SM.3 of Supplementary Material, it was verified that the kinetic data presented here were obtained under chemical regime. The catalyst stability was verified by performing two consecutive reactions with a negligible difference between both CH consumption rates (Section SM.4 of Supplementary Material).

Considering the catalyst characterization, catalytic activity results, and previous reports from literature [2,5], the proposed heterogeneous LHHW kinetic models were based on the following hypothesis and assumptions:

(a) The only reaction products are CHMPE and CHMP.
(b) Both CHMPE and CHMP are primary products and the former can be isomerized into the latter.
(c) The catalyst contains a single type of acid site.
(d) The rate limiting step for OA and CA are the same at the light that both reactants are in contact with the catalyst from zero time.
(e) Surface chemical reactions forming CHMPE and CHMP are irreversible.
(f) CHMP product does not adsorb on the sites.

The general system of differential equations representing the mass balance of the species is presented in Eqs. (4)–(7):

$$\frac{dC^*_{CH}}{dt} = \frac{1}{C^0_G} \cdot \frac{dC_{CH}}{dt} = \frac{1}{C^0_G} \cdot \left(-r_{OA} - r_{CA} \right) = -r^*_{OA} - r^*_{CA} \tag{4}$$

$$\frac{dC^*_G}{dt} = \frac{1}{C^0_G} \cdot \frac{dC_G}{dt} = \frac{1}{C^0_G} \cdot \left(-r_{OA} - r_{CA} \right) = -r^*_{OA} - r^*_{CA} \tag{5}$$

$$\frac{dC^*_{CHMPE}}{dt} = \frac{1}{C^0_G} \cdot \frac{dC_{CHMPE}}{dt} = \frac{1}{C^0_G} \cdot \left(r_{OA} - r_I \right) = r^*_{OA} - r^*_I \tag{6}$$

$$\frac{dC^*_{CHMP}}{dt} = \frac{1}{C^0_G} \cdot \frac{dC_{CHMP}}{dt} = \frac{1}{C^0_G} \cdot \left(r_{OA} - r_I \right) = r^*_{CA} + r^*_I \tag{7}$$

where $C^*_i = \frac{C_i}{C^0_G}$ is the relative concentration of compound i and $r^*_j = \frac{r_j}{C^0_G}$ is the modified reaction rate corresponding to reaction j.
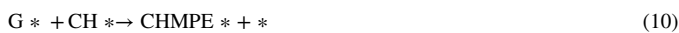
Considering the former hypothesis, the elementary steps shown in Eqs. (8)–(13) represent the general reaction mechanism, where * is an active acid site:

$$G+ * \leftrightarrow G* \tag{8}$$

Table 1

LHHW kinetic models used in the study.

N°	Rate limiting steps	r_i expressions
1	OA: ADS CH CA: ADS CH I: ADS CHMPE	$r_{OA} = \dfrac{C_S^T \cdot k_{CH} \cdot C_{CH}}{(1 + K_G \cdot C_G)}$ $r_{CA} = \dfrac{C_S^T \cdot k_{CH} \cdot C_{CH}}{(1 + K_G \cdot C_G)}$ $r_I = \dfrac{C_S^T \cdot k_{CHMPE} \cdot C_{CHMPE}}{(1 + K_G \cdot C_G)}$
2	OA: ADS CH CA: ADS CH I: SCR	$r_{OA} = \dfrac{C_S^T \cdot k_{CH} \cdot C_{CH}}{(1 + K_G \cdot C_G + K_{CHMPE} \cdot C_{CHMPE})}$ $r_{CA} = \dfrac{C_S^T \cdot k_{CH} \cdot C_{CH}}{(1 + K_G \cdot C_G + K_{CHMPE} \cdot C_{CHMPE})}$ $r_I = \dfrac{C_S^T \cdot k_{SR-I} \cdot K_{CHMPE} \cdot C_{CHMPE}}{(1 + K_G \cdot C_G + K_{CHMPE} \cdot C_{CHMPE})}$
3	OA: SCR CA: SCR I: SCR	$r_{OA} = \dfrac{(C_S^T)^2 \cdot k_{SR-OA} \cdot K_{CH} \cdot K_G \cdot C_{CH} \cdot C_G}{(1 + K_{CH} \cdot C_{CH} + K_G \cdot C_G + K_{CHMPE} \cdot C_{CHMPE})^2}$ $r_{CA} = \dfrac{(C_S^T)^2 \cdot k_{SR-CA} \cdot K_{CH} \cdot K_G \cdot C_{CH} \cdot C_G}{(1 + K_{CH} \cdot C_{CH} + K_G \cdot C_G + K_{CHMPE} \cdot C_{CHMPE})^2}$ $r_I = \dfrac{C_S^T \cdot k_{SR-I} \cdot K_{CHMPE} \cdot C_{CHMPE}}{(1 + K_{CH} \cdot C_{CH} + K_G \cdot C_G + K_{CHMPE} \cdot C_{CHMPE})}$
4	OA: SCR CA: SCR I: ADS CHMPE	$r_{OA} = \dfrac{(C_S^T)^2 \cdot k_{SR-OA} \cdot K_{CH} \cdot K_G \cdot C_{CH} \cdot C_G}{(1 + K_{CH} \cdot C_{CH} + K_G \cdot C_G)^2}$ $r_{CA} = \dfrac{(C_S^T)^2 \cdot k_{SR-CA} \cdot K_{CH} \cdot K_G \cdot C_{CH} \cdot C_G}{(1 + K_{CH} \cdot C_{CH} + K_G \cdot C_G)^2}$ $r_I = \dfrac{C_S^T \cdot k_{CHMPE} \cdot C_{CHMPE}}{(1 + K_{CH} \cdot C_{CH} + K_G \cdot C_G)}$

OA: O-alkylation; CA: C-alkylation; I: isomerization; SCR: surface chemical reaction; ADS i: adsorption of i.

$$CH + * \leftrightarrow CH* \tag{9}$$

$$G* + CH* \rightarrow CHMPE* + * \tag{10}$$

$$G* + CH* \rightarrow CHMP + 2* \tag{11}$$

$$CHMPE* \rightarrow CHMP + * \tag{12}$$

$$CHMPE* \leftrightarrow CHMPE + * \tag{13}$$

Taking into account several possibilities for the rate limiting steps and adsorption, four different LHHW-like models were developed. The mathematical expressions for the reaction rates corresponding to these LHHW models are presented in Table 1.

The expressions for the O-alkylation, C-alkylation and isomerization reaction rates (r_{OA}, r_{CA} and r_I) in Table 1 were simplified by grouping kinetic (k), equilibrium constants (K) and total concentration of active sites (C_S^T) as parameters P_j, where j identifies the group of constants. These simplified expressions, the estimated parameters with their intervals with a confidence level of 95% and the statisticals S, r^2 and MSC are presented in Table 2.

The fitting with Model 1 was satisfactory ($S = 9.43 \times 10^{-4}$) and provided positive estimates for the parameters. However, considering a 95% confidence level the estimates for P_1, P_2 and P_3 were non-significantly different from zero (Table 2). In other words, the estimated parameters have physical meaning but no statistical significance, thus Model 1 was rejected.

Model 2 fitted experimental data satisfactorily ($S = 8.63 \times 10^{-4}$) and also provided positive estimates for all the parameters (Table 2). Nevertheless, none of the parameters had statistical significance because the left borders of the confidence intervals were negative and therefore

Model 2 was rejected. At the light of this, and assuming saturated catalytic surface ($\Sigma K_i \cdot C_i \gg 1$) a new Model 2.a was developed and tested. Model 2.a fitted data better ($S = 6.72 \times 10^{-4}$) than Model 2, though P_2 estimate (K_{CHMPE}/K_G) was negative (Table 2), which is meaningless from a physical point of view. For these reasons, Model 2 and Model 2.a were also rejected.

Model 3 performed considerably better at fitting experimental data ($S = 2.38 \times 10^{-4}$) than Models 1 and 2 but not only a negative value for the P_4 estimate (K_{CHMPE}) which does not make any sense from a physical point of view, but also estimates not significantly different from zero (Table 2) were obtained. As in the case of Model 2, an alternative Model 3.a was developed by assuming saturated catalytic surface ($\Sigma K_i \cdot C_i \gg 1$). Although the fitting of Model 3.a was even better than Model 3 ($S = 2.31 \times 10^{-4}$), the P_3 estimate for the ratio K_{CHMPE}/K_G was negative. In consequence, Model 3 and Model 3.a were also discarded.

In the case of Model 4, the fitting was very good ($S = 2.40 \times 10^{-4}$) and all the estimates of the parameters were positive. However, all the estimates were not significantly different from 0 (Table 2). By assuming saturated catalytic surface ($\Sigma K_i \cdot C_i \gg 1$) and low coverage of CH ($K_{CH} \cdot C_{CH} \cong 0$) the Model 4.a was developed. Although the fitting of experimental value with Model 4.a was satisfactory ($S = 8.56 \times 10^{-4}$), this model did not fit experimental data as well as Model 4 but gave positive estimates and significantly different from 0 for all the parameters.

Finally, assuming only saturated catalytic surface ($\Sigma K_i \cdot C_i \gg 1$) and dividing numerator and denominator by K_G in the r_i expressions of Model 4, the Model 4.b was generated, which fitted the experimental data much better than Model 4.a ($S = 2.40 \times 10^{-4}$). Furthermore, Model 4.b provided positive estimates for all the parameters and significantly different from 0, as well.

Comparing the results with Model 4.a and 4.b it is possible to see that the objective function S is lower with Model 4.b and, although Model 4.b has one parameter more, the *MSC* was appreciable higher. Thus, the best model among the LHHW models tested in this work was Model 4.b. The fitting of the experimental data with Model 4.a and 4.b and the residuals ($C_{i,t}^* - C_{i,t}^{*CALC}$) are shown in Fig. 3. From Fig. 3.a it is clear that Model 4.b fits experimental very well, showing absolute residuals ($C_{i,t}^* - C_{i,t}^{*CALC}$) always lower than 8×10^{-3} (Fig. 3.b), which corresponds to relative residuals of 0.8% or less.

Finally, it is worth noticing that the parameter P_2 in Model 4.b is the $\frac{K_{CH}}{K_G}$ ratio; which means that K_{CH} is almost twice the value of K_G, suggesting a stronger CH adsorption over acid sites.

Based on these findings, a mechanism for the alkylation reaction in these experimental conditions between an adsorbed G molecule and an adsorbed CH molecule over acid sites in Amberlyst 36 is proposed in Fig. 4. The adsorption and protonation of cyclohexene on the acidic sites of the catalyst generate the cyclohexyl cation (electrophile) which reacts with guaiacol by attacking the oxygen of the hydroxyl group (O-alkylation) or through the π electrons of the aromatic ring (C-alkylation) leading to the formation of CHMPE and the different CHMP isomers, respectively [16]. The CHMPE may further adsorb on catalyst surface to isomerize to the final product CHMP.

4. Conclusions

The kinetics of the heterogeneous liquid-phase alkylation of guaiacol with cyclohexene over Amberlyst 36 sulfonic acid resin has been studied in this work. The LHHW model that fits experimental data satisfactorily and provides parameter estimates with physical and statistical meaning predicts that: (a) both O-alkylated and C-alkylated compounds are primary reaction products; (b) the rate limiting step for the O-alkylation and C-alkylation is the surface chemical reaction between and adsorbed cyclohexene and guaiacol molecules; (c) O-alkylation products are converted into C-alkylation products by isomerization where the adsorption of O-alkylation product is the rate limiting step; (d) the adsorption constant of cyclohexene is almost twice the value than for guaiacol.

Table 2
Results of the LHHW kinetic modeling.

| N°	Simplified r_i expressions	Parameters	Estimated parameters, confidence intervals and statisticals
1	$r_{OA} = \dfrac{P_1 \cdot C_{CH}}{(1 + P_2 \cdot C_G)}$ $r_{CA} = \dfrac{P_1 \cdot C_{CH}}{(1 + P_2 \cdot C_G)}$ $r_I = \dfrac{P_3 \cdot C_{CHMPE}}{(1 + P_2 \cdot C_G)}$	$P_1 = C_S^T \cdot k_{CH}$ $P_2 = K_G$ $P_3 = C_S^T \cdot k_{CHMPE}$	P_1=81.03 [-2382.5/2544.6] P_2=228.07 [-6737.7/7193.9] P_3=394.14 [-11536.5/12324.8] S=9.43×10^{-4} r²=0.9998 MSC=8.56
2	$r_{OA} = \dfrac{P_1 \cdot C_{CH}}{(1 + P_2 \cdot C_G + P_3 \cdot C_{CHMPE})}$ $r_{CA} = \dfrac{P_1 \cdot C_{CH}}{(1 + P_2 \cdot C_G + P_3 \cdot C_{CHMPE})}$ $r_I = \dfrac{P_4 \cdot C_{CHMPE}}{(1 + P_2 \cdot C_G + P_3 \cdot C_{CHMPE})}$	$P_1 = C_S^T \cdot k_{CH}$ $P_2 = K_G$ $P_3 = K_{CHMPE}$ $P_4 = C_S^T \cdot k_{SR-I} \cdot K_{CHMPE}$	P_1=57.15 [-1051.9/1166.2] P_2=112.1 [-2078.5/2302.8] P_3=23.15 [-422.5/468.8] P_4=284.47 [-5245.3/5814.3] S=8.63×10^{-4} r²=0.9998 MSC=8.60
2.a	$r_{OA} = \dfrac{P_1 \cdot C_{CH}}{(C_G + P_2 \cdot C_{CHMPE})}$ $r_{CA} = \dfrac{P_1 \cdot C_{CH}}{(C_G + P_2 \cdot C_{CHMPE})}$ $r_I = \dfrac{P_3 \cdot C_{CHMPE}}{(C_G + P_2 \cdot C_{CHMPE})}$	$P_1 = \dfrac{C_S^T \cdot k_{CH}}{K_G}$ $P_2 = \dfrac{K_{CHMPE}}{K_G}$ $P_3 = \dfrac{C_S^T \cdot k_{SR-I} \cdot K_{CHMPE}}{K_G}$	P_1=0.26 [0.23/0.29] P_2= -14.30 [-19.00/-9.60] P_3=1.06 [0.85/1.27] S=6.72×10^{-4} r²=0.9999 MSC=8.90
3	$r_{OA} =$ $\dfrac{P_1 \cdot C_{CH} \cdot C_G}{(1 + P_2 \cdot C_{CH} + P_3 \cdot C_G + P_4 \cdot C_{CHMPE})^2}$ $r_{CA} =$ $\dfrac{P_5 \cdot C_{CH} \cdot C_G}{(1 + P_2 \cdot C_{CH} + P_3 \cdot C_G + P_4 \cdot C_{CHMPE})^2}$ $r_I =$ $\dfrac{P_6 \cdot C_{CHMPE}}{(1 + P_2 \cdot C_{CH} + P_3 \cdot C_G + P_4 \cdot C_{CHMPE})}$	$P_1 =$ $(C_S^T)^2 \cdot k_{SR-OA} \cdot K_{CH} \cdot K_G$ $P_2 = K_{CH}$ $P_3 = K_G$ $P_4 = K_{CHMPE}$ $P_5 =$ $(C_S^T)^2 \cdot k_{SR-CA} \cdot K_{CH} \cdot K_G$ $P_6 = C_S^T \cdot k_{SR-I} \cdot K_{CHMPE}$	P_1=1.40 [-19.57/22.37] P_2=4.05 [-16.81/24.92] P_3=0.28 [-11.32/11.88] P_4= -2.18 [-21.81/17.45] P_5=1.08 [-15.28/17.45] P_6=3.62 [-23.44/30.68] S=2.38×10^{-4} r²=0.9999 MSC=9.82
3.a	$r_{OA} =$ $\dfrac{P_1 \cdot C_{CH} \cdot C_G}{(P_2 \cdot C_{CH} + C_G + P_3 \cdot C_{CHMPE})^2}$ $r_{CA} =$ $\dfrac{P_4 \cdot C_{CH} \cdot C_G}{(P_2 \cdot C_{CH} + C_G + P_3 \cdot C_{CHMPE})^2}$ $r_I = \dfrac{P_5 \cdot C_{CHMPE}}{(P_2 \cdot C_{CH} + C_G + P_3 \cdot C_{CHMPE})}$	$P_1 = \dfrac{(C_S^T)^2 \cdot k_{SR-OA} \cdot K_{CH}}{K_G}$ $P_2 = \dfrac{K_{CH}}{K_G}$ $P_3 = \dfrac{K_{CHMPE}}{K_G}$ $P_4 = \dfrac{(C_S^T)^2 \cdot k_{SR-CA} \cdot K_{CH}}{K_G}$ $P_5 = \dfrac{C_S^T \cdot k_{SR-I} \cdot K_{CHMPE}}{K_G}$	P_1=0.56 [0.40/0.72] P_2=1.69 [1.18/2.20] P_3= -2.45 [-5.98/1.07] P_4=0.43 [0.29/0.57] P_5=2.30 [1.62/2.96] S=2.31×10^{-4} r²=0.9999 MSC=9.88
4	$r_{OA} = \dfrac{P_1 \cdot C_{CH} \cdot C_G}{(1 + P_2 \cdot C_{CH} + P_3 \cdot C_G)^2}$ $r_{CA} = \dfrac{P_4 \cdot C_{CH} \cdot C_G}{(1 + P_2 \cdot C_{CH} + P_3 \cdot C_G)^2}$ $r_I = \dfrac{P_5 \cdot C_{CHMPE}}{(1 + P_2 \cdot C_{CH} + P_3 \cdot C_G)}$	$P_1 =$ $(C_S^T)^2 \cdot k_{SR-OA} \cdot K_{CH} \cdot K_G$ $P_2 = K_{CH}$ $P_3 = K_G$ $P_4 =$ $(C_S^T)^2 \cdot k_{SR-CA} \cdot K_{CH} \cdot K_G$ $P_5 = C_S^T \cdot k_{CHMPE}$	P_1=1.52 [-10.83/13.87] P_2=4.20 [-8.50/16.91] P_3=0.29 [-5.83/6.41] P_4=15.15 [-8.10/10.40] P_5=3.81 [-11.94/19.55] S=2.40×10^{-4} r²=0.9999 MSC=9.84
4.a	$r_{OA} = \dfrac{P_1 \cdot C_{CH}}{C_G}$ $r_{CA} = \dfrac{P_2 \cdot C_{CH}}{C_G}$ $r_I = \dfrac{P_3 \cdot C_{CHMPE}}{C_G}$	$P_1 = \dfrac{(C_S^T)^2 \cdot k_{SR-OA} \cdot K_{CH}}{K_G}$ $P_2 = \dfrac{(C_S^T)^2 \cdot k_{SR-CA} \cdot K_{CH}}{K_G}$ $P_3 = \dfrac{C_S^T \cdot k_{CHMPE}}{K_G}$	P_1=0.48 [0.30/0.66] P_2=0.22 [0.04/0.41] P_3=2.38 [1.25/3.52] S=8.56×10^{-4} r²=0.9998 MSC=8.66
4.b	$r_{OA} = \dfrac{P_1 \cdot C_{CH} \cdot C_G}{(P_2 \cdot C_{CH} + C_G)^2}$ $r_{CA} = \dfrac{P_3 \cdot C_{CH} \cdot C_G}{(P_2 \cdot C_{CH} + C_G)^2}$ $r_I = \dfrac{P_4 \cdot C_{CHMPE}}{(P_2 \cdot C_{CH} + C_G)}$	$P_1 = \dfrac{(C_S^T)^2 \cdot k_{SR-OA} \cdot K_{CH}}{K_G}$ $P_2 = \dfrac{K_{CH}}{K_G}$ $P_3 = \dfrac{(C_S^T)^2 \cdot k_{SR-CA} \cdot K_{CH}}{K_G}$ $P_4 = \dfrac{C_S^T \cdot k_{CHMPE}}{K_G}$	P_1=0.64 [0.51/0.77] P_2=1.91 [1.45/2.38] P_3=0.48 [0.33/0.63] P_4=2.48 [1.83/3.13] S=2.40×10^{-4} r²=0.9999 MSC=9.88
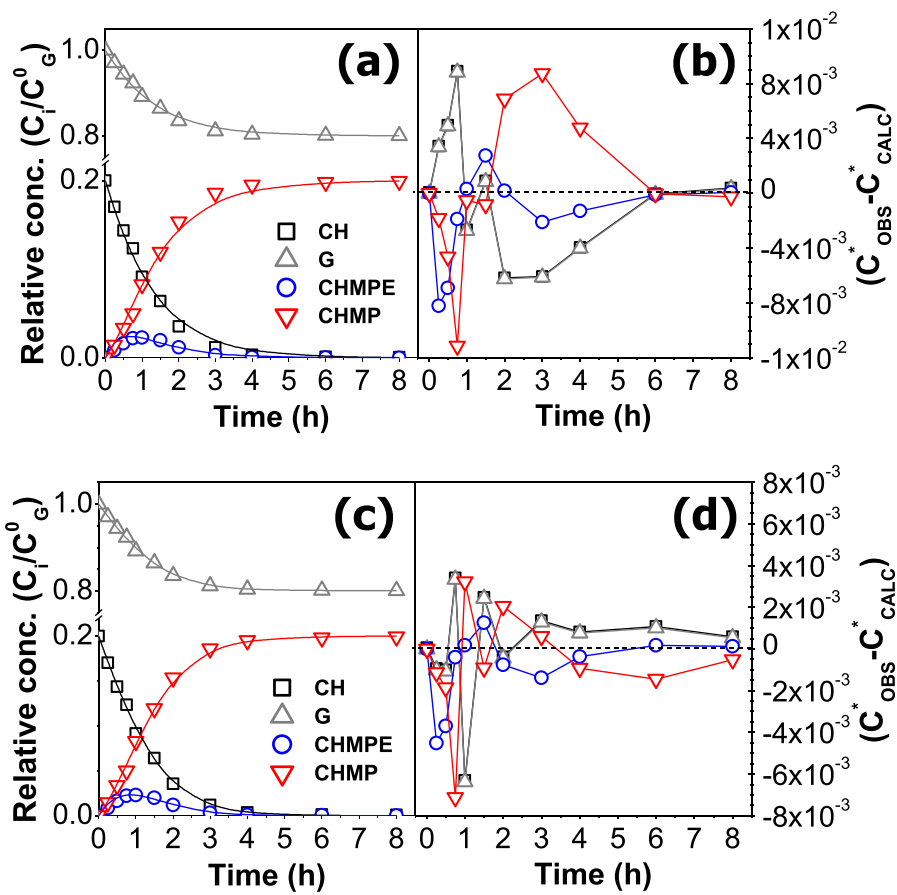
Fig. 3. Results of the kinetic modeling using Models 4.a (a,b) and 4.b (c,d): (a,c) experimental (symbols) and modeling prediction (full lines); (b,d) residuals for CH, G, CHMPE and CHMP [363 K, C_{CAT} = 50 g/L, G:CH 5:1 molar].
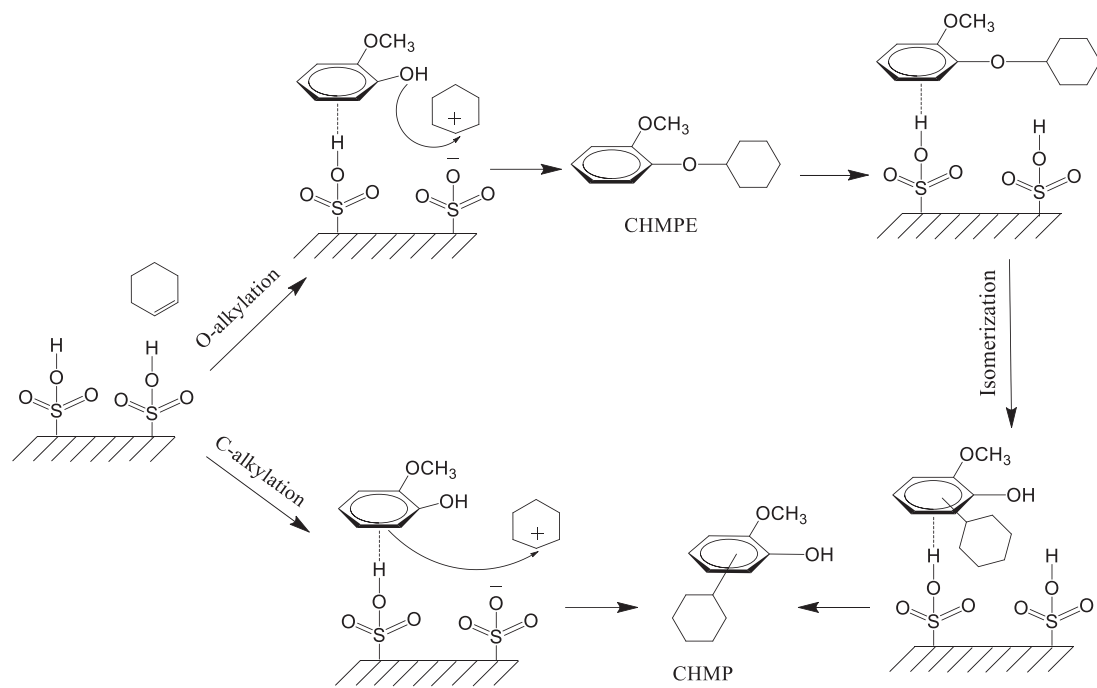

Fig. 4. Proposed mechanism for the alkylation of G with CH on Amberlyst 36 based on the kinetic modeling results.

Declaration of Competing Interest

The authors declare that they have no known competing financial interests or personal relationships that could have appeared to influence the work reported in this paper.

Acknowledgments

Supplementary materials

Supplementary material associated with this article can be found, in the online version, at doi:10.1016/j.ceja.2021.100112.

References

[1] A. Corma, H. García, Lewis acids: from conventional homogeneous to green homogeneous and heterogeneous catalysis, Chem. Rev. 103 (2003) 4307–4366, doi:10.1021/cr030680z.

[2] G.D. Yadav, G.S. Pathre, Chemoselective catalysis by sulphated zirconia in O-alkylation of guaiacol with cyclohexene, J. Mol. Catal. A Chem. 243 (2006) 77–84, doi:10.1016/j.molcata.2005.08.024.

[3] G.D. Yadav, G.S. Pathre, Selectivity engineering of cation-exchange resins over inorganic solid acids in C-alkylation of guaiacol with cyclohexene, Ind. Eng. Chem. Res. 46 (2007) 3119–3127, doi:10.1021/ie060645t.

[4] J.M. Lavoie, W. Baré, M. Bilodeau, Depolymerization of steam-treated lignin for the production of green chemicals, Bioresour. Technol. 102 (2011) 4917–4920, doi:10.1016/j.biortech.2011.01.010.

[5] P.de Wild, R.Van der Laan, A. Kloekhorst, E. Heeres, Lignin valorisation for chemicals and (Transportation) fuels via (Catalytic) pyrolysis and hydrodeoxygenation, Environ. Prog. Sustain. Energy 28 (2009) 461–469, doi:10.1002/ep.10391.

[6] Y. Nakagawa, M. Ishikawa, M. Tamura, K. Tomishige, Selective production of cyclohexanol and methanol from guaiacol over Ru catalyst combined with MgO, Green Chem. 16 (2014) 2197–2203, doi:10.1039/c3gc42322k.

[7] G.D. Yadav, G.S. Pathre, Chemoselective catalysis by sulphated zirconia in O-alkylation of guaiacol with cyclohexene, J. Mol. Catal. A Chem. 243 (2006) 77–84, doi:10.1016/j.molcata.2005.08.024.

[8] L.R. Pizzio, M.N. Blanco, A contribution to the physicochemical characterization of nonstoichiometric salts of tungstosilicic acid, Microporous Mesoporous Mater. 103 (2007) 40–47, doi:10.1016/j.micromeso.2007.01.036.

[9] P.A. Ramachandran, R.V. Chaudhari, Three-Phase Catalytic Reactors, Gordon and Breach Science Publishers, 1983.

[10] P.B. Weisz, C.D. Prater, Interpretation of measurements in experimental catalysis, Adv. Catal. 6 (1954) 143–196.

[11] N.M. Bertero, A.F. Trasarti, M.C. Acevedo, A.J. Marchi, C.R. Apesteguía, Solvent effects in solid acid-catalyzed reactions: The case of the liquid-phase isomerization/cyclization of citronellal over SiO$_2$-Al$_2$O$_3$, Mol. Catal. 481 (2020) 11019–110209, doi:10.1016/j.mcat.2018.09.009.

[12] N.M. Bertero, C.R. Apesteguía, A.J. Marchi, Liquid-phase dehydration of 1-phenylethanol over HZSM-5: Kinetic modeling, Catal. Commun. 10 (2009) 1339–1344, doi:10.1016/j.catcom.2009.02.018.

[13] A. Eftaxias, J. Font, A. Fortuny, A. Fabregat, F. Stüber, Nonlinear kinetic parameter estimation using simulated annealing, Comput. Chem. Eng. 26 (2002) 17251733, doi:10.1016/S0098-1354(02)00156-4.

[14] Z. Belohlav, P. Zamostny, P. Kluson, J. Volf, Application of random-search algorithm for regression analysis of catalytic hydrogenations, Can. J. Chem. Eng. 75 (1997) 735–742, doi:10.1002/cjce.5450750411.

[15] P. Zamostny, Z. Belohlav, A software for regression analysis of kinetic data, Comput. Chem. 23 (1999) 479–485, doi:10.1016/S0097-8485(99)00024-8.

[16] M.E. Sad, C.L. Padró, C.R. Apesteguía, Synthesis of cresols by alkylation of phenol with methanol on solid acids, Catal. Today 133–135 (2008) 720–728, doi:10.1016/j.cattod.2007.12.074.